*American Mineralogist, Volume 104, pages 615–618, 2019*

**LETTER**

# Synthesis of pigeonites for spectroscopic studies

**DONALD H. LINDSLEY[1,*], HANNA NEKVASIL[1], AND TIMOTHY D. GLOTCH[1]**

[1]Department of Geosciences, Stony Brook University, ESS Building, 100 Nicholls Road, Stony Brook, New York 11794-2100, U.S.A.

## ABSTRACT

Pigeonite ($P2_1/c$ clinopyroxene) crystallizes in various terrestrial and extraterrestrial rocks. However, because it breaks down ("inverts") in slowly cooled rocks, bulk natural samples of pigeonite from coarse-grained rocks are not available. We have synthesized eight samples of pigeonite with compositions of $Wo_8$ and $Wo_{10}$ [where Wo (mol%) = $100Ca/(Ca+Mg+Fe^{2+})$] and $X$ ranging from 20 to 60 [where $X = 100Fe^{2+}/(Mg+Fe^{2+})$]. These samples are suitable for spectroscopic and other studies that require bulk samples. Because of relatively fine grain size (mainly 5–50 μm) and slight grain-to-grain variation in composition, they are generally not suitable for studies requiring individual crystals. We will make samples available for appropriate investigations, especially if the techniques used are non-destructive and the samples can be returned after use.

**Keywords:** Pigeonite, synthesis, clinopyroxene, bulk samples, spectroscopy

## INTRODUCTION

Pigeonite, i.e., clinopyroxene containing approximately 10% Wo [where the amount of Wo (at%) = $100Ca/(Ca+Mg+Fe^{2+})$], is reported from terrestrial, lunar, and planetary samples (e.g., Basaltic Volcanism Study Project 1981, p. 65, 184, and 224). It forms in various igneous and high-temperature metamorphic rocks but survives as a discrete phase almost exclusively in rapidly cooled, fine-grained lavas. This is because pigeonite has a minimum thermal stability temperature below which, upon slow cooling, it breaks down ("inverts") to an intergrowth of augite lamellae in an orthopyroxene host—the so-called "inverted pigeonite" texture. Since pigeonite does not survive as a discrete phase in plutonic rocks, and it is tedious to separate pigeonite grains from the fine-grained lavas in which they do survive, we lack natural pigeonite for measurements that require bulk samples. To remedy this, we have synthesized eight samples of pigeonite to serve as standards for spectroscopic and other studies.

Synthesis of pigeonite is complicated by several characteristics of phase equilibria in the pyroxene quadrilateral. Pigeonite synthesis must take place within its stability field, that is, above the temperature of its minimum thermal stability (e.g., Fig. 6 of Davidson and Lindsley 1985) but below the solidus temperature in the pure $Ca_2Si_2O_6$-$Mg_2Si_2O_6$-$Fe_2Si_2O_6$ system (Fig. 4b of Huebner and Turnock 1980; our Fig. 1). Thus, for a given $X$ [$X = 100Fe^{2+}/(Fe^{2+}+Mg)$ molar], there is a relatively narrow temperature window for successful synthesis. Furthermore, as both the minimum pigeonite stability and solidus temperatures decrease with increasing $X$, this window shifts with composition. Much early work concentrated on making pigeonite in the Fe-free (Kushiro 1969; Yang 1973; Schweitzer 1982; Tribaudino et al. 2002) and Mg-free (Lindsley 1981) joins. Turnock et al. (1973) reported the synthesis of pigeonite at a wide variety of $X$ and listed several techniques for synthesis. They used their Method 1 (controlled-gas, quench furnace, 1 atm) to make pigeonites with $X$ ranging from 20 to 60, and their Method 5 (hydrothermal synthesis at 2 GPa) for pigeonite with $X = 75$ (because pigeonite of that composition lies in the "Forbidden Zone" and is not stable at 1 bar, e.g., Lindsley 1983). Neither method, however, is well suited for making gram-quantities of pigeonite, so we used a modification of their Method 2: synthesis in sealed, evacuated silica-glass tubes, to allow us to process 1 to 3 g of material in each tube. We aimed to make ~5 g of each composition, with Wo values of 8 and 10, and $X$ ranging from 20 (few natural pigeonites are more magnesian than this) to 60 (near the edge of the "Forbidden Zone" and thus near the limit for synthesis at low pressure).

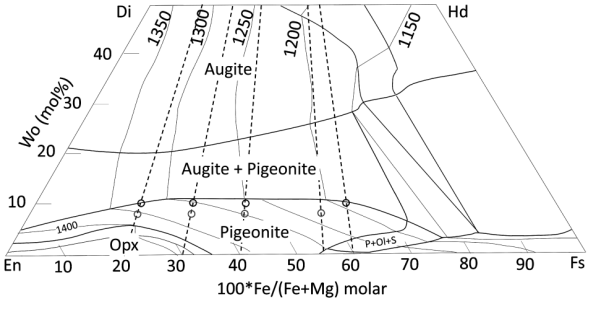


**FIGURE 1.** Solidus diagram for Ca-Mg-$Fe^{2+}$ pyroxenes at 1 atm (adopted from Huebner and Turnock 1980; their Fig. 4b), showing the approximate pigeonite field and the target compositions for our work (open circles). Wo (mol%) = $Ca_2Si_2O_6$, or $100Ca/(Ca+Mg+Fe^{2+})$; $X = 100Fe^{2+}/(Mg+Fe^{2+})$ (at%); En = $Mg_2Si_2O_6$; Fs = $Fe_2Si_2O_6$; Di = $CaMgSi_2O_6$; Hd = $CaFeSi_2O_6$; Opx = orthopyroxene; Ol = olivine; S = silica phase (tridymite, cristobalite, or quartz). We omit labels for the complex region near Hd and Fs. Note that olivine has higher $X$ than the coexisting pigeonite, as shown by the composition of olivine coexisting with pigeonite at the solidus.

* E-mail: donald.lindsley@stonybrook.edu

## Synthesis details

### Starting materials

All initial mixes were made from stoichiometric quantities of dried $CaSiO_3$, MgO, $SiO_2$ (quartz), $Fe_2O_3$, and $Fe^0$ sponge. We used hematite and iron sponge as the source of FeO because stoichiometric FeO is not stable. We measured the amount of oxygen in the $Fe^0$ sponge (see p. 52 of Turnock et al. 1973; also Supplementary[1] Materials) and adjusted the amount of hematite used accordingly to yield the desired bulk FeO content. All components except the $Fe^0$ sponge were ground together under ethanol for several hours in an automatic agate mortar; to minimize oxidation, the sponge was added only for the last 30–40 min of grinding.

Previous experience had shown that placing the original starting mix directly into the pigeonite stability field yields pigeonite riddled with inclusions of intermediate phases (augite, olivine, and silica); and because those intermediate phases were "armored" within pigeonite, the reaction among them became extremely slow. We avoided most of that difficulty by "pre-reacting" the starting materials at 900–920 °C, a temperature range below the minimum stability of pigeonite (details in Supplementary Materials[1]). The pre-reacted starting material for the pigeonite synthesis consisted of crystalline augite, olivine, and quartz.

### Final synthesis

Pre-reacted materials were packed into iron capsules machined to 2 to 4 cm in length with snugly fitting lids from medium-purity (99.6 to 99.95%) ¼ inch (6.35 mm) OD rod. The loaded capsules were placed in 7 mm ID silica-glass tubes, dried under vacuum at 800 °C for 10 min using an iron "oxygen getter" ($Fe^0$ sponge) placed in the tubes at ~600 °C to prevent oxidation, and the tubes were then sealed under vacuum. We used two heating approaches for the synthesis. The first involved holding the sample at a fixed temperature below the solidus for direct synthesis in the solid state. The second approach involved partially melting the sample at ~25–50 °C above the solidus temperature, then cooling it slowly to below the solidus temperature, and finally holding the sample at that lower temperature, with the goal of using the presence of melt to speed up the reaction and to grow larger crystals. Unfortunately, most samples treated using this second approach were strongly zoned, with low-Ca, high-Mg cores mantled by rims close to the target composition. Only one sample treated in this way ($Wo_{10}$ $X$ = 60 T) was sufficiently homogeneous to be acceptable (Fig. 2). Samples are named by the target composition plus a letter (A, B, etc.) designating the sequence of that sample in the synthesis attempts for that composition.

All but one sample ($Wo_8$ $X$ = 40 E) underwent more than one stage of "final" synthesis: the products of previous attempts were re-heated (usually with intermediate grinding) to produce more nearly homogeneous materials. Details are in Supplemental[1] Table S1. Especially for more magnesian compositions that required higher temperatures, run durations were nerve-wracking compromises between the desire to maximize reaction time and the knowledge that the enclosing silica-glass tubes would eventually fail because of softening and/or devitrification. Because of the recycling and associated losses of material (when the silica-glass tubes failed and samples within them became oxidized), the samples reported here fall short of the 5 g target by varying amounts.

### Characterization of materials

We characterized the synthesis products optically (both under a binocular microscope and immersed in refractive-index oil

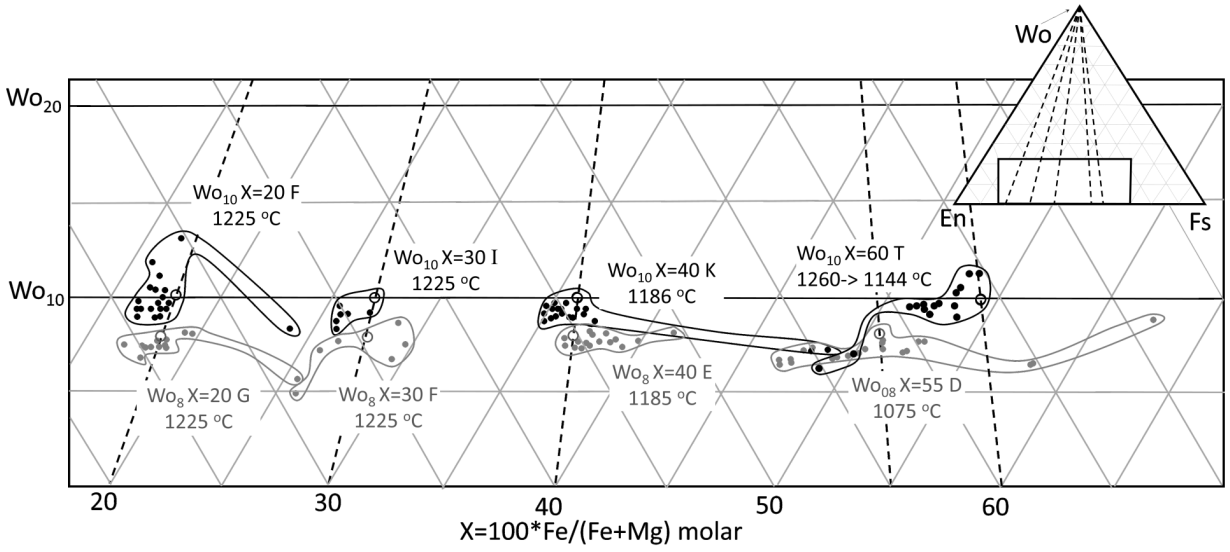


**Figure 2.** Portion of the pyroxene quadrilateral showing target compositions (open circles) and microprobe analyses (solid points; Supplemental[1] Table S2) of the samples. All analyses with close to $(Mg+Fe+Ca)_2Si_2O_6$ stoichiometry [Si = 1.98 to 2.02; Ca+Mg+Fe(+Mn) = 1.98–2.02] are plotted. MnO (generally <O.6 and more commonly <0.3 wt%) was added to FeO to form Fs component. Black symbols and text refer to $Wo_{10}$ samples; gray to $Wo_8$. We deliberately searched for and report outlier compositions to show diversity of grain compositions. For this reason the bulk compositions of the samples are best represented by the clusters of analyses near the target compositions, not an average of the points shown. See text for interpretation of outlier points. Components as in caption to Figure 1.

under a petrographic microscope), with powder X-ray diffraction; and by electron microprobe. Optical examination showed mainly pigeonite; small amounts of a silica phase; rare olivine inclusions (where noted in Table 1); and residual quenched melt (one sample). Because syntheses were performed in iron capsules, all samples contain iron metal (<0.1 to 0.9 wt% $Fe^0$), as inclusions and/or discrete grains.

**X-ray diffraction.** We used Stony Brook's Rigaku Miniflex system with Cu radiation, scanning from 18° to 128° 2θ for our powder XRD analyses. Diffraction data were processed with the software on "Match!3" (Crystal Impact 2016) to identify phases, compute their proportions, and to refine the pigeonite cell parameters (Table 1). Pigeonite dominated in the assemblage produced; however, most samples also showed small amounts (0.5 to 2 wt%) of unreacted silica. Although tridymite is considered the stable polymorph of $SiO_2$ at the conditions of synthesis, only one sample showed tridymite. Mg-rich compositions (which required higher synthesis temperatures) produced mainly cristobalite; Fe-rich ones contained quartz, presumably inherited from the starting material.

Our unit-cell parameters (Table 1) agree moderately well with values predicted by the equations of Morrison et al. (2018) (Pigeonite: $P2_1/c$ in the box, top of their p. 852). Although there is some variation, their predicted values average 0.008 Å lower than our measured values for $a$, 0.006 Å lower for $b$, 0.0004 Å lower for $c$, and 0.09° higher for β. Measured and calculated values are shown in Supplemental[1] Table S2.

**Microprobe analysis.** The goal for quantitative compositional analysis was to report the widest observed range of compositions. Standards used in EMPA were anorthite for Ca, San Carlos olivine for Mg; fayalite for Fe, and Lake County plagioclase for Si. Analysis conditions were 1 μm nominal beam size, 15 keV accelerating voltage, and 20 nA beam current. Because the samples are saturated with iron metal, we assume that virtually all the iron structurally in the pigeonite is $Fe^{2+}$. Owing to the small grain size of most samples, most analyses aimed for the centers of the grains and the search for minor phases and zoning within pigeonite was restricted to backscattered electron imaging. We report (Fig. 2; Supplemental[1] Table S3) all analyses that totaled 98–102 wt% and approached $M_2Si_2O_6$ stoichiometry (Si 1.98–2.02; divalent cations 1.98–2.02 per 6 O atoms). For three samples (Wo8 $X$ = 30 G; Wo8 $X$ = 30 F; Wo8 $X$ = 40 E) we had to accept sums lower than 98%, in part because of fine grain size. Most analyses for most samples cluster close to (but are slightly more Mg-rich than) the target compositions. Mg-rich outliers most likely reflect zoning within pigeonite; those with higher Fe and lower Ca than the intended bulk composition probably overlap onto olivine inclusions (olivine that coexists with pigeonite has higher values of $X$; see Fig. 1); and those with higher Ca and higher Fe almost certainly represent overlap with the quenched melt. Although the final temperatures of synthesis were always below the solidus (Fig. 1) the pre-reacted starting material was not the stable assemblage at $T$, therefore, metastable melting was a possibility, and some of this melt may have survived the prolonged soak at the subsolidus $T$. Please note that because we deliberately searched for and report outlier compositions, the range of compositions in Figure 2 is almost certainly not representative of the bulk composition of the sample, which is best approximated by the clustered analyses. That conclusion is bolstered by the relatively sharp peaks in the X-ray diffraction patterns.

## IMPLICATIONS

Because bulk samples of natural pigeonites are not available, synthetic samples are needed for various studies. However, synthesis of gram-quantities of pigeonite remains difficult. The eight samples reported here are products of the most successful of more than 125 synthesis attempts over several years. Potential users of these samples should be aware of the within-sample variations; the samples should be used for studies on bulk samples. As any individual grain may deviate considerably from the nominal composition, we do not recommend using individual crystals unless each crystal has been analyzed by microprobe.

Those who wish to obtain samples for specific studies should contact T.D. Glotch, (timothy.glotch@stonybrook.edu), stating the composition(s) desired, which measurements will be made; optimum and minimum quantities needed; and whether the sample(s) can be returned undamaged and uncontaminated after use. Requesters should take into account: (1) the widely varying amounts available for each sample, (2) that some samples are more nearly uniform in composition than others, and (3) that there are variations in grain size. Preference will be given to those who will use nondestructive techniques. Please note that the sample names include both the target compositions and the letter (e.g., A, B, C) that uniquely designates the particular sample. (For example, the sample name $Wo_{10}$ $X$ = 60 T implies that there are

**TABLE 1.** Synthesized pigeonites

| Target comp.[a] | Sample letter | Synthesis $T$ (°C) | ~Grams available | Grain size (μm) | Yield (wt%) Pigeonite | Yield (wt%) Other phases[b] | Cell parameters ($P2_1/c$)[c] $a$ (Å) | $b$ (Å) | $c$ (Å) | β (°) | $V$ (Å$^3$) |
|---|---|---|---|---|---|---|---|---|---|---|---|
| Wo8 X = 20 | G | 1225 | 0.4 | 25–50 | 98 | cr (2); ol (tr) | 9.6774(4) | 8.8881(4) | 5.2197(2) | 108.4808(36) | 425.815(6) |
| Wo10 X = 20 | F | 1225 | 4 | 5–50 | >99 | cr (0.5); ol (tr) | 9.6851(3) | 8.8907(3) | 5.2263(2) | 108.439(3) | 426.918(7) |
| Wo8 X = 30 | F | 1225 | 0.8 | 5–10 | >99 | cr (0.7) | 9.6832(4) | 8.9047(3) | 5.2242(2) | 108.521(3) | 426.985(8) |
| Wo10 X = 30 | I | 1225 | 2.6 | 5–50 | >99 | trid (0.6) | 9.6918(5) | 8.9084(4) | 5.2300(2) | 108.487(4) | 428.246(7) |
| Wo8 X = 40 | E | 1185 | 4 | 5–10 | >99 | qtz (0.9) | 9.6960(4) | 8.9315(3) | 5.2322(2) | 108.553(3) | 429.564(7) |
| Wo10 X = 40 | K | 1186 | 1.6 | 5–30 | >99 | cr (0.6); ol (tr) | 9.7058(4) | 8.9363(3) | 5.2393(2) | 108.496(3) | 430.950(8) |
| Wo8 X = 55 | D | 1075 | 0.37 | 5–10 | >99 | qtz (0.6); gl (tr) | 9.7082(5) | 8.9677(4) | 5.2403(3) | 108.545(4) | 432.528(7) |
| Wo10 X = 60 | T | 1260; 1144 | 0.7 | 80–120 | >99 | gl (tr) | 9.724(1) | 8.987(1) | 5.2492(9) | 108.38(2) | 435.33(2) |

*Notes*: Because syntheses were done in $Fe^0$ capsules, all samples contain metallic iron. Match! reports <0.1 to 0.9 wt% $Fe^0$. Details of each synthesis are in Supplementary materials.

[a] Wo = 100Ca/(Ca+Mg+Fe). X = 100Fe/(Mg+Fe) atomic.

[b] cr = cristobalite; trid = tridymite; qtz = quartz; ol = olivine; gl = glass or quenched melt; tr = trace (seen optically or inferred from outlier probe analyses).

[c] Values in parentheses show 1σ uncertainty in last significant figure, calculated by multiplying the formal uncertainty of the refinement by the Berar "Score", typically ~4 to 6.

at least 19 other samples (A...S) of that target composition! The T is essential for identifying that sample.) The letter designator must be retained in all reports that use the sample.

## Funding

This work was supported by the RIS⁴E node of NASA's Solar System Exploration Research Virtual Institute (T.D.G.) and by NSF grant EAR1725212 (H.N.).

## Acknowledgments

This paper is dedicated to the fond memory of Allan Charles Turnock (1930–2018), colleague and close friend of D.H.L. since student days. Samples were analyzed using the Cameca SX-100 probe at the American Museum of Natural History (New York). We thank Nicholas DiFrancesco, Douglas Schaub, and Tristan Catalano for their careful work in probing these challenging samples, and Adrian Fiege for helping them. Alexandra Sinclair contributed to early stages of the project. We thank Mario Tribaudino, Stephen Huebner, and an anonymous reviewer for their timely and helpful reviews.

## References cited

Basaltic Volcanism Study Project (1981) Basaltic Volcanism on the Terrestrial Planets, 1286 pp. Pergamon Press.

Davidson, P.M., and Lindsley, D.H. (1985) Thermodynamic analysis of quadrilateral pyroxenes. Part II: Model calibration from experiments and applications to geothermometry. Contributions to Mineralogy and Petrology, 91, 390–404.

Huebner, J.S., and Turnock, A.C. (1980) The melting relations at 1 bar of pyroxenes composed largely of Ca-, Mg-, and Fe-bearing components. American Mineralogist, 65, 225–271.

Kushiro, I. (1969) The system forsterite-diopside-silica with and without water at high pressures. American Journal of Science, 267-A (Schairer Volume), 269–294.

Lindsley, D.H. (1981) The formation of pigeonite on the join hedenbergite-ferrosilite at 11.5 and 15 kbar: Experiments and a solution model. American Mineralogist, 66, 1175–1182.

——— (1983) Pyroxene thermometry. American Mineralogist, 68, 477–493.

Morrison, S.M., Downs, R.T, Blake, D.F., Prabhu, A., Eleish, A., Vaniman, D.T., Ming, D.W., Rampe, E.B., Hazen, R.M., Achilles, C.N., and others (2018) Relationships between unit-cell parameters and composition for rock-forming minerals on Earth, Mars, and other extraterrestrial bodies. American Mineralogist, 103, 848–856.

Crystal Impact (2016) Match!—Phase Identification from Powder Diffraction, ver. 3. Crystal Impact, Bonn, Germany. http://www.crystalimpact.com/match.

Schweitzer, E.J. (1982) The reaction pigeonite = $diopside_{ss}$ + $enstatite_{ss}$ at 15 kbars. American Mineralogist, 67, 54–58.

Tribaudino, M., Nestola, F., Cámara, F., and Domeneghetti, M.C. (2002) The high temperature $P2_1/c$-$C2/c$ phase transition in Fe-free pyroxene ($Ca_{0.15}Mg_{1.85}Si_2O_6$): structural and thermodynamic behavior. American Mineralogist, 87, 648–657.

Turnock, A.C., Lindsley, D.H., and Grover, J.E. (1973) The synthesis and unit-cell parameters of Ca-Mg-Fe pyroxenes. American Mineralogist, 58, 50–59.

Yang, H.-Y. (1973) Crystallization of iron-free pigeonite in the system anorthite-diopside-enstatite-silica at atmospheric pressure. American Journal of Science, 273, 488–497.

Manuscript received November 2, 2018
Manuscript accepted December 1, 2018
Manuscript handled by Ian Swainson

## Endnote

[1]Deposit item AM-19-46869, Supplemental Material and Tables. Deposit items are free to all readers and found on the MSA web site, via the specific issue's Table of Contents (go to http://www.minsocam.org/MSA/AmMin/TOC/2019/Apr2019_data/Apr2019_data.html).